Acta Crystallographica Section A
Foundations of Crystallography
ISSN 0108-7673

Received 21 April 2003
Accepted 9 September 2003

The fine structure of X-ray diffuse scattering in the vicinity of high-angle superlattice Bragg reflections

V. A. Chernov,[a] N. V. Kovalenko,[b] S. V. Mytnichenko[c]* and A. I. Toropov[d]

[a]Boreskov Institute of Catalysis, Siberian SR Center at Budker Institute of Nuclear Physics, 630090 Novosibirsk, Russia, [b]Budker Institute of Nuclear Physics, 630090 Novosibirsk, Russia, [c]Institute of Solid State Chemistry, Siberian SR Center at Budker Institute of Nuclear Physics, 630090 Novosibirsk, Russia, and [d]Institute of Semiconductor Physics, 630090 Novosibirsk, Russia. Correspondence e-mail: s.v.mytnichenko@inp.nsk.su

Triple-axis X-ray diffractometry was used to study diffuse scattering from an AlAs/GaAs superlattice grown on an [001]-oriented GaAs substrate by molecular beam epitaxy. Reciprocal-space maps were obtained around the 002 reflection from the superlattice and its low-angle first-order satellite. The data obtained reveal quasi-Bragg diffuse-scattering sheets caused by conformal behavior of interfacial roughness as well as amplification of diffuse scattering when the incoming or outgoing angle is nearly equal to the Bragg angle of the superlattice or substrate. The observed features of diffuse-scattering fine structure are explained within the framework of the distorted-wave Born approximation. Nevertheless, this approximation is shown to be incorrect for quantitative analysis of diffuse scattering. In particular, the observed domination in intensity of the incoming Bragg features over the outgoing ones is shown to reflect the decay rate of the coherent X-ray field through the diffuse-scattering channel, which is not negligible relative to the coherent diffraction.

1. Introduction

X-ray diffuse scattering from multilayers and superlattices has been the subject of many studies in the last decade. Significant scientific progress in X-ray diffuse scattering from amorphous multilayers was made at that time. It started with studies (Andreev *et al.*, 1988; Bruson *et al.*, 1989; Savage *et al.*, 1991; Kortright, 1991; Stearns, 1992) where coherent replication of rough multilayer interfaces was shown to cause resonant amplification of diffuse scattering, resulting in observation of 'quasi-Bragg' diffuse scattering. Another diffraction effect is resonant amplification of diffuse scattering when the incoming or outgoing angle is nearly equal (within Darwin's table) to the Bragg angle. This effect was observed experimentally for the first time by Kortright & Fischer-Colbrie (1987), Savage *et al.* (1991) and Kortright (1991). It was qualitatively explained as a standing-wave effect for the incident and diffusely scattered X-ray fields. Numerical theoretical calculations of the phenomenon under discussion were performed by extending the distorted-wave Born approximation (DWBA), previously used to calculate diffuse scattering from single surfaces by Sinha *et al.* (1988), to the case of multilayers (Holý & Baumbach, 1994; Kopecky, 1995).

The case of X-ray diffuse scattering from superlattices is more complicated. One of the most important reasons for that is the inevitable presence of a terrace structure (Gibaud *et al.*, 1993; Sinha *et al.*, 1994; Headrick *et al.*, 1995; Jenichen *et al.*, 1996; Kondrashkina *et al.*, 1997; Darhuber, Zhu *et al.*, 1998; Holý, Darhuber, Stangl, Bauer *et al.*, 1998; Clarke *et al.*, 1999). As a result, both interfacial roughness and lattice strain become anisotropic in the lateral directions, which leads to observation of diffuse-scattering dependence on the azimuthal sample orientation. In the case of small-angle Bragg reflections from multilayers, diffuse scattering is caused only by electron-density fluctuations at interfaces (interfacial roughness). In contrast to that, in the case of lattice Bragg reflections from superlattices and their satellites, diffuse scattering is also caused by variations in lattice strain depending on lateral coordinates. Furthermore, in contrast to the case of non-epitaxic multilayers, replication of interfacial profiles across the layer stack can be more intricate in superlattices (Headrick *et al.*, 1995; Jenichen *et al.*, 1996; Holý, Darhuber, Stangl, Bauer *et al.*, 1998). Nevertheless, the interest in the diffuse-scattering method increased recently, particularly in connection with creation of novel semiconductor devices such as quantum dots or wires (Darhuber *et al.*, 1995, 1996, 1997; Giannini *et al.*, 1997; Darhuber, Holy *et al.*, 1998; Holý, Darhuber, Stangl, Zerlauth *et al.*, 1998; Holý *et al.*, 2000; Zhuang *et al.*, 2000).

In this article, we report our results of a high-resolution X-ray diffraction study of diffuse-scattering fine structure in the vicinity of a high-angle Bragg reflection from an AlAs/GaAs superlattice. In §2, DWBA is used to perform qualitative analysis of diffuse scattering. The generalized analytic expression for the diffuse-scattering cross section is obtained, which allows us to classify clearly the fine-structure features of

diffuse scattering in the vicinity of high-angle superlattice Bragg reflections. These features are the quasi-Bragg, quasi-specular, incoming and outgoing Bragg scattering. In §3, the experimental conditions are described. In §4, the experimental data obtained are presented and discussed. DWBA is shown to be acceptable for the qualitative description of diffuse scattering only. The quantitative calculation of the diffuse-scattering cross section needs to take into account the multiple diffuse-scattering events.

2. Distorted-wave Born approximation

In order to calculate X-ray scattering from any object, it is necessary to solve the wave equation

$$(\Delta + k^2)E(\mathbf{r}) = V(\mathbf{r})E(\mathbf{r}), \quad (1)$$

where $k = 2\pi/\lambda$ is the wavevector, $V(\mathbf{r}) = 4\pi r_0 \rho(\mathbf{r})$ is the scattering potential, r_0 is the classical electron radius, $\rho(\mathbf{r})$ is the electron density and $E(\mathbf{r})$ is the solution. Here, σ polarization of the incident beam is implied, which allows us to exclude the polarization of waves from consideration. Since the wavevector of a diffusely scattered X-ray photon slightly differs from that of a specular reflected wave, the equation obtained can be easily extended to the case of π polarization by using the usual polarization factor.

DWBA can be applied to solve equation (1) if it is possible to split the scattering potential into two nonequivalent parts:

$$V(\mathbf{r}) = V_0(\mathbf{r}) + \Delta V(\mathbf{r}),$$

where $V_0(\mathbf{r})$ is the basic potential, for which solutions of the wave equation are known, and $\Delta V(\mathbf{r})$ is a small perturbation. Within the framework of these presumptions, the scattering amplitude can be written in the following form (Taylor, 1972):

$$f(\mathbf{k}_0 \rightarrow \mathbf{k}_1) = f_0(\mathbf{k}_0 \rightarrow \mathbf{k}_1) + \frac{1}{4\pi}\langle E, \mathbf{k}_1 - |\Delta V(\mathbf{r})| E, \mathbf{k}_0\rangle, \quad (2)$$

where $f_0(\mathbf{k}_0 \rightarrow \mathbf{k}_1)$ is the amplitude of scattering from the potential $V_0(\mathbf{r})$ of the incoming plane wave with vector $\mathbf{k}_0$ into the outgoing plane wave with vector $\mathbf{k}_1$ and $|E, \mathbf{k}_0\rangle \equiv E_{\mathbf{k}_0}$ is the solution of (1) with $V(\mathbf{r}) = V_0(\mathbf{r})$ for the incident plane wave with vector $\mathbf{k}_0$. The state $|E, \mathbf{k}_1 -\rangle$ is more intricate. If photoabsorption and inelastic scattering, which cause dissipation of coherent wave energy, are neglected, the state $|E, \mathbf{k}_1 -\rangle$ is a time-inverted solution for the incident plane wave with the vector $-\mathbf{k}_1$. Note that time inversion of the state is equivalent to complex conjugation of the state. Thus,

$$|E, \mathbf{k}_1 -\rangle \equiv E^*_{-\mathbf{k}_1}.$$

Expression (2) for the scattering amplitude allows one to obtain the differential cross section of scattering

$$\frac{d\sigma}{d\Omega} = |f(\mathbf{k}_0 \rightarrow \mathbf{k}_1)|^2. \quad (3)$$

Applying DWBA to the case of diffraction from superlattices with rough interfaces, it is natural to define $V_0(z)$ as the laterally symmetrical part of the whole potential

$$V_0(z) = \langle V(\mathbf{r})\rangle_{x,y},$$

where x, y are the lateral axes and z is the axis normal to the lateral planes (Fig. 1). Note that values of the momentum-transfer projections on the lateral plane of diffusely scattered X-rays are small relative to the reciprocal superlattice vectors, which allows one not to take into account the periodicity of $V(\mathbf{r})$ at the atomic scale lengths in lateral directions. Correspondingly, the perturbation part of the potential can be defined as

$$\Delta V(\mathbf{r}) = V(\mathbf{r}) - V_0(z).$$

The diffuse-scattering amplitude can be calculated from the second term of equation (2):

$$\Delta f(\mathbf{k}_0 \rightarrow \mathbf{k}_1) = \frac{1}{4\pi}\int E_{\mathbf{k}_0} E_{-\mathbf{k}_1} \Delta V(\mathbf{r})\, d\mathbf{r}. \quad (4)$$

Equation (4) transforms into the well known Born approximation if the incoming and outgoing angles (Fig. 1) are far from the Bragg angle. In this case, $E_{\mathbf{k}_0} \cong \exp(i\mathbf{k}_0\mathbf{r})$, $E_{-\mathbf{k}_1} \cong \exp(-i\mathbf{k}_1\mathbf{r})$ and $\Delta V(\mathbf{r}) = 4\pi r_0 \Delta\rho(\mathbf{r})$, which allows one to obtain

$$\Delta f(\mathbf{k}_0 \rightarrow \mathbf{k}_1) = r_0 \int \Delta\rho(\mathbf{r}) \exp(-i\mathbf{q}\cdot\mathbf{r})\, d\mathbf{r},$$

where $\mathbf{q} = \mathbf{k}_1 - \mathbf{k}_0$ is the momentum transfer.

Let the solutions of (1) with $V = V_0$ be known and able to be written in the following form:

$$|E, \mathbf{k}_0\rangle = E_{\mathbf{k}_0} = [T_0(z)\exp(ik_{0z}z) + R_0(z)\exp(-ik_{0z}z)] \times \exp(ik_{0x}x + ik_{0y}y),$$

where $T_0(z)$ and $R_0(z)$ are slowly varying functions of z corresponding to the amplitudes of the transmitted and specularly reflected waves, and then the conjugate state can be written as

$$|E, \mathbf{k}_1 -\rangle = E^*_{-\mathbf{k}_1} = [T_1^*(z)\exp(ik_{1z}z) + R_1^*(z)\exp(-ik_{1z}z)] \times \exp(ik_{1x}x + ik_{1y}y).$$

Substitution of these forms of states in (4) and (3) gives the following expression for the diffuse-scattering cross section:

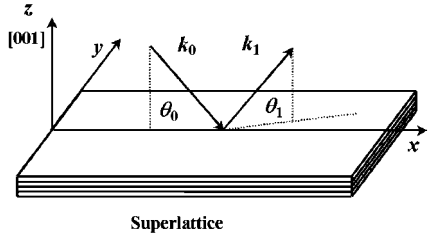

Figure 1
Geometry of the diffuse-scattering experiment: the axis z is normal to the lateral planes; the lateral axis x lies in the specular diffraction plane defined by the incident and specularly reflected wavevectors; the lateral axis y is normal to this plane (azimuthal direction); $\mathbf{k}_0$ is the wavevector of the incident plane wave; $\mathbf{k}_1$ is the wavevector of the diffusely scattered wave; θ_0 and θ_1 are the incoming and outgoing angles, respectively.

$$\frac{d\sigma}{d\Omega} = r_0^2 \left| \int \Delta\rho(\mathbf{r})[T_0 T_1 \exp(-iq_z z) + R_0 T_1 \exp(-i\kappa z) + T_0 R_1 \exp(i\kappa z) + R_0 R_1 \exp(iq_z z)] \times \exp(-iq_x x - iq_y y)\, d\mathbf{r} \right|^2, \quad (5)$$

where $\kappa = k_{0z} + k_{1z}$. Note that the expression obtained is valid for the superlattice Bragg reflections as well as for the substrate Bragg reflections. There is some difference that the spatial locations of $V_0(\mathbf{r})$ and $\Delta V(\mathbf{r})$ do not intersect in the first case, but this difference is not principal. The degree of coherence of $V_0(\mathbf{r})$ and $\Delta V(\mathbf{r})$ is much more important.

Expression (5) allows one to perform a physically clear classification of diffuse-scattering features, which can be observed in the reciprocal space near the specular Bragg reflections. First, it is necessary to note that the first three terms in (5) describe the appearance of diffuse scattering in various regions of the reciprocal space, excluding some specific regions such as a Bragg point.

2.1. Quasi-Bragg diffuse scattering

The first term $T_0 T_1$ in (5) describes the diffuse scattering that can be calculated in the Born approximation if $T_0(z) \cong T_1(z) \cong 1$. It is well known that the conformal behavior of interfacial roughness through the layer stack of the multilayer causes resonant amplification of diffuse scattering generating a quasi-Bragg sheet in the reciprocal space near the small-angle Bragg reflections from multilayers (Andreev *et al.*, 1988; Bruson *et al.*, 1989; Savage *et al.*, 1991; Kortright, 1991; Stearns, 1992). In this case, the condition of quasi-Bragg diffuse scattering can be written as

$$q_z \approx Q, \quad (6)$$

where $Q = 2\pi/\Lambda$ is the reciprocal-space vector and Λ is the period of the multilayer. The reason for this scattering can be explained easily taking into account the translation symmetry of potential $\Delta V(\mathbf{r})$ with vector $\mathbf{\Lambda}$.

Obviously, a similar effect occurs in the case of high-angle Bragg reflections from superlattices with the same resonant condition as equation (6). In contrast to the case of small-angle Bragg reflection, there are two interconnected origins of $\Delta V(\mathbf{r})$ in this case. The first origin is interfacial roughness, which is the same as in the case of small-angle Bragg reflections. The second origin is variations in the lattice strain depending on lateral coordinates. Though the second origin is caused by the first one, their influence on diffuse scattering near the basic lattice Bragg reflection and its satellite is different. Only strain variations can provide the appearance of a quasi-Bragg sheet near the basic lattice reflections. As for the superlattice satellites, both interfacial roughness and strain variations are important.

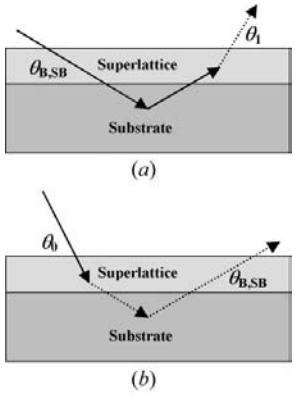

Figure 2
Origin of the (*a*) incoming and (*b*) outgoing Bragg features in the case of Bragg reflection from the substrate.

Thus, coherent replication of interfacial roughness and strain variations from one bilayer to another causes resonant amplification of diffuse scattering, resulting in the appearance of a quasi-Bragg sheet in the reciprocal space. The extent of quasi-Bragg diffuse scattering in the q_z direction, Δq_z, is the same as for the specular Bragg reflection if the interfacial roughness is completely correlated through the layer stack. Otherwise, if the roughness is partially correlated in the vertical direction, this value is greater compared to the specular Bragg reflection (Stearns, 1992). It is quite evident that the degree of vertical correlation depends on a lateral length scale of roughness. At large scales, the roughness must be completely correlated (Stearns, 1992). At the same time, the contribution from the longer scale roughness to the diffuse-scattering cross section dominates (de Boer, 1996). Thus, the use of a conventional experimental technique with the integration of diffuse-scattering intensity over q_y provides the fact that the value of Δq_z depends weakly on q_x and is approximately the same as for the case of specular Bragg reflection. This effect was observed repeatedly for small-angle Bragg reflection from multilayers (Gullikson *et al.*, 1997; Chernov *et al.*, 2000).

The resonant amplification discussed provides domination of the contribution of the conformal part of $\Delta V(\mathbf{r})$ to the diffuse-scattering cross section over that of the non-conformal part of $\Delta V(\mathbf{r})$. Substitution of the non-conformal part of $\Delta V(\mathbf{r})$ in the first term of (5) gives a diffuse halo around the Bragg point. Spread of this halo in the reciprocal space is defined by the mean sizes of roughness defects in the real space.

2.2. Incoming and outgoing Bragg scattering.

The second and third terms in (5) provide resonant amplification of diffuse scattering forming the incoming and outgoing Bragg features when the amplitude R_0 or R_1 reaches maximum or when

$$\theta_0 \approx \theta_B \quad \text{or} \quad \theta_1 \approx \theta_B,$$

where θ_0, θ_1 are the incoming and outgoing angles (Fig. 1), respectively, and θ_B is the Bragg angle. The breadth of the incoming and outgoing Bragg features in the q_z direction are defined by the R amplitude. Thus, as in the case of quasi-Bragg scattering, the profiles of the incoming and outgoing Bragg features in the q_z direction are replicated from the specular reflectivity curve, but with the corresponding translation in this direction *versus* q_x.

The origin of the features discussed can be explained especially easily in the case of a Bragg reflection from the substrate. There may be two different orders of scattering events (Fig. 2). In the first case, the primary beam with the substrate's Bragg angle of incidence is reflected by the substrate and then the reflected beam is diffusely scattered by the superlattice, generating the incoming Bragg feature (Fig. 2*a*). However, the order of the events can be inverted. In spite of the angle of incidence of the primary beam, the small-angle diffuse scattering is effectively reflected if its angle of incidence on the substrate is nearly equal to the substrate's Bragg angle, generating the outgoing Bragg feature (Fig. 2*b*). These processes are of a dynamical nature because the incoming and outgoing features are visible if the substrate's Bragg reflectivity is not vanishingly small. Moreover, the standing-wave and other dynamical effects can play an important role in diffraction if the sources of diffuse scattering [potential $\Delta V(\mathbf{r})$] in the superlattice are located coherently relative to the substrate lattice. A similar explanation can be found for the superlattice features. Although it is impossible to separate the scattering events in time so clearly as in the case of the substrate's Bragg peak, the basic physical mechanism of this phenomenon is the same.

In contrast to the previous case of quasi-Bragg scattering, it is quite easy to show with (5) that the contribution of the conformal part $\Delta V(\mathbf{r})$ to the intensity of the incoming and outgoing Bragg features is effectively dumped. Thus, the non-conformal interfacial roughness can play an important role in the case of incoming and outgoing Bragg scattering.

In connection with the features discussed, it is necessary to consider the influence of the standing-wave effect on diffuse scattering. Let us assume that the angle of incidence is such that the nodes of the standing wave are located at the interfaces of the superlattice. Then, in this case, diffuse scattering must be dumped and one can observe breaks in diffuse-scattering intensity (Kortright & Fischer-Colbrie, 1987). Nevertheless, the term R_0T_1 alone evidently cannot provide these breaks. The discussed effect appears if the interference of the terms R_0T_1 and T_0T_1 is included, which is not surprising because the standing wave is caused by interference of T_0 and R_0 waves. Experimental observation of the standing-wave effect near the Bragg point is evidently difficult owing to the domination of the specular reflectivity signal in this case. Nevertheless, it is easy to perform this in the regions of the reciprocal space, where the quasi-Bragg and incoming (or outgoing) Bragg features of different Bragg orders intersect (Savage *et al.*, 1991; Kortright, 1991; Jergel *et al.*, 1995; Kaganer *et al.*, 1995).

2.3. Quasi-specular diffuse scattering.

It is not so clear as in the previous case that the second and third terms in (5) generate another type of resonant diffuse scattering. It is quasi-specular diffuse scattering (Chernov *et al.*, 2002).[1] Indeed, in spite of the fact that, according to the definition, $\langle \Delta V(\mathbf{r}) \rangle = 0$ the amplitude $R(z)$ is an approximately linear function of z if the angle of incidence is quite far from the Bragg angle and $\int z \Delta V(\mathbf{r}) \mathrm{d}z \neq 0$. Thus, if the condition

$$\theta_0 \approx \theta_1 \quad \text{or} \quad \kappa = k_{0z} + k_{1z} \approx 0 \tag{7}$$

is met, there must be resonant amplification of diffuse scattering. Note that this scattering is not true specular scattering because (7) is not exact and imposes no constraint on the values of q_x and q_y. The resonance condition $\kappa\tau < 1$, where τ is the total thickness of superlattices in the case of superlattice Bragg reflection or the wave extinction depth in the case of substrate Bragg reflection, allows one to estimate the spreading of quasi-specular feature in the q_x direction:

$$\Delta q_x \sim \frac{\tan\theta_0}{\tau}.$$

Thus, quasi-specular diffuse scattering occurs in a very narrow (in the q_x direction) region near the true specular signal in the reciprocal space. The usual measurements with integration of intensity in the q_y direction (Fig. 1) do not allow one to observe clearly this type of diffuse scattering. The use of azimuthal experimental schemes with the measurements of diffuse scattering intensity *versus* q_y (Kortright & Fischer-Colbrie, 1987; Salditt *et al.*, 1994; Salditt, Metzger, Brandt *et al.*, 1995; Salditt, Metzger, Peisl *et al.*, 1995; Salditt *et al.*, 1996) allows one to overcome this problem (Chernov *et al.*, 2002).

In contrast to the previous case, the non-conformal part of $\Delta V(\mathbf{r})$ does not give a contribution to the cross section of quasi-specular diffuse scattering.

In the vicinity of the Bragg point in the reciprocal space, all the four terms of (5) interfere, forming a complicated structure. An experimental study of this structure is beyond the scope of the present work owing to evident difficulties, the most important being domination of specular (and quasi-specular) reflection intensity.

3. Experimental

An $[(AlAs)_{9ML}/(GaAs)_{9ML}] \times 80$ superlattice was grown by molecular beam epitaxy on a [001]-oriented GaAs substrate with a buffer AlAs layer (~50 nm) in the Riber 32P system. The growth was monitored by reflection high-energy electron diffraction. The sample was characterized by X-ray diffraction using Cu $K\alpha$ radiation from a conventional X-ray source. A theoretical simulation of diffraction data obtained has allowed us to conclude that the structure of the sample was practically perfect.

X-ray diffuse-scattering measurements were performed using synchrotron radiation (SR) from the VEPP-3 storage ring and a triple-axis diffractometer with a primary channel-cut single-crystal Si(111) monochromator and a Ge(111) crystal collimator at the wavelength λ = 0.154 nm. The measurements were performed in the vertical plane so that the crystal–monochromator, specimen and secondary crystal–collimator were placed in the (+,+,+) geometry. The measured vertical angular broadening of the diffractometer had a full width at half-maximum (FWHM) of 15″. As for the horizontal

[1] A mention of this effect can be found also in Sinha *et al.* (1994).

plane, the horizontal size of the incident beam was about 1 mm and no secondary collimators for the scattered radiation were used. Thus, the intensity of diffuse scattering was integrated in the azimuthal (horizontal) direction. A scintillation detector based on an FEU-130 photomultiplier with an NaI(Tl) scintillator was used. The dynamic range of the detector system was about 2×10^4. Calibrated copper foils were used to increase the dynamic range of measurements.

The measured value of the miscut angle was found to be about 0.23° and the miscut direction was slightly (~5°) off the [110] direction. The main diffuse-scattering measurements were performed in such way that the specular diffraction plane defined by the incident and reflected wavevectors was along the [110] crystallographic direction across the terrace steps.

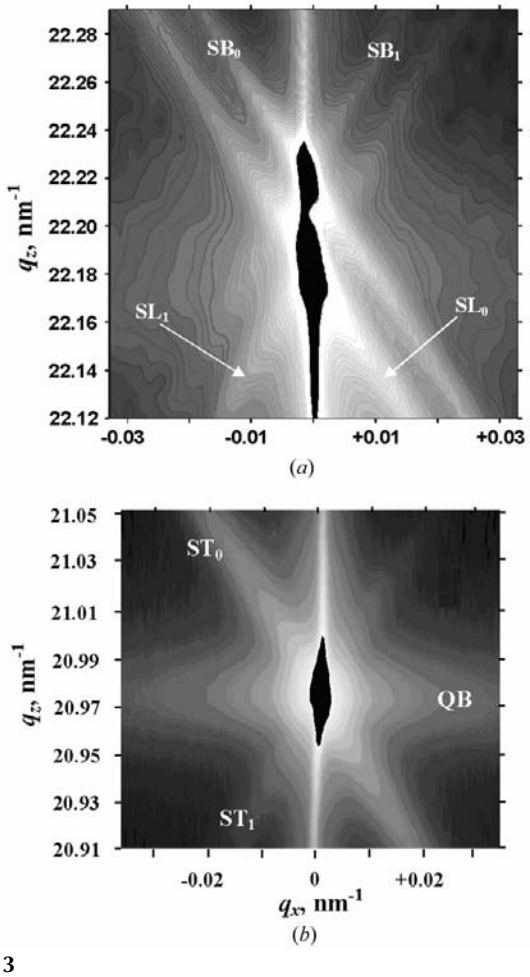

Figure 3
Diffraction maps of (*a*) the 002 reflection and (*b*) its low-angle first-order satellite. The in-plane projection of the momentum transfer is plotted parallel to the horizontal axis. The momentum transfer projection, normal to the lateral planes, is plotted parallel to the vertical axis. The intensity is shown on the logarithmic scale. Although the dynamical range of the measurements was about 10^6, in order to show clearly the diffuse-scattering fine structure, the high-intensity points were cut, which caused the final dynamical range of the maps to be about 10^4. The reported diffuse-scattering features are presented as inclined streaks. Features $SB_{0,1}$ and $SL_{0,1}$ correspond to the basic Bragg reflection from the substrate and superlattice, respectively. The features $ST_{0,1}$ correspond to the satellite Bragg peak. Their indices correspond to two conditions when the incoming or outgoing angle, respectively, is equal to the Bragg angle. The feature marked as QB is the quasi-Bragg diffuse scattering.

4. Results and discussion

Diffraction maps of the 002 reflection and its first-order low-angle satellite are shown in Fig. 3. These maps were obtained as a set of transverse scans (ω scans, $\theta_0 + \theta_1 = \text{constant}$). The vertical streaks in the maps correspond to the specular and quasi-specular scattering. A horizontal sheet in Fig. 3(*b*) corresponds to the quasi-Bragg diffuse scattering. It is marked as QB. A similar feature can be seen in the upper map. Although the quasi-Bragg scattering intensity in this case is comparable to the case of satellite reflection, its relative value compared to specular reflection intensity is remarkably smaller. This fact is illustrated in Fig. 4, where the intensities of the specular and off-specular scans are compared. As was discussed in §2, this behavior of the quasi-Bragg scattering means that contribution of strain variations to the diffuse-scattering cross section is quite low. It is not surprising because the epitaxic mismatch of AlAs and GaAs lattices is small.

The incoming and outgoing Bragg features are marked as SL_0 and SL_1, corresponding to the superlattice Bragg angle, as SB_0 and SB_1, corresponding to the substrate Bragg angle, and as ST_0 and ST_1, corresponding to the satellite Bragg angle. First, it is necessary to note that mapping of the 002 reflection from the original substrate does not reveal any inclined streaks. Moreover, besides the discussed features, the diffuse-scattering intensity signal in this case was, at least, 10–100 times smaller compared to the case of the superlattice. It allows us to conclude that the observed inclined streaks are not caused by some experimental failures.

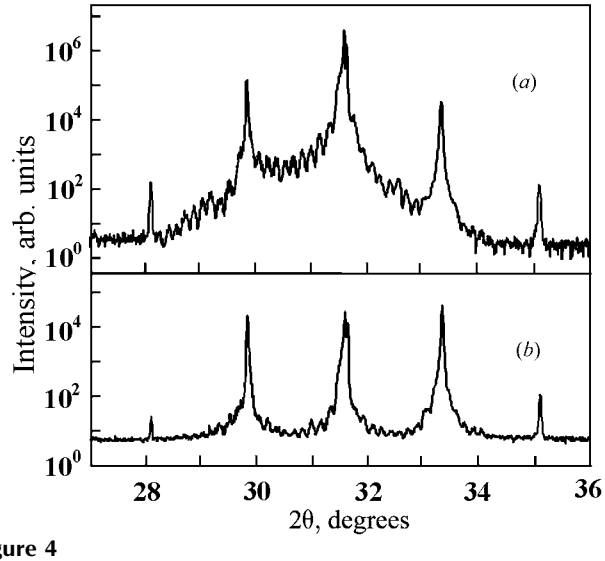

Figure 4
(*a*) Specular ($\theta - 2\theta$) and (*b*) off-specular [$(\theta + \Delta\theta) - 2\theta$, $\Delta\theta = 0.002°$] scans through the 002 reflection and its first- and second-order satellites. Note that the intensities of the diffuse scattering (*b*) are approximately equal for the basic reflection and its first-order satellites. At the same time, intensity of specular reflection (*a*) is almost ten times greater compared to the satellites. The oscillations in the intensities are caused by diffraction from the buffer layer.

It is easy to see that cross section (5) is symmetrical relative to the interchanging of indexes $0 \leftrightarrow 1$. That is not accidental. Indeed, matrix element (4) can be considered as the scattering amplitude $\Delta f(\mathbf{k}_0 \rightarrow \mathbf{k}_1)$ as well as the scattering amplitude $\Delta f(-\mathbf{k}_1 \rightarrow -\mathbf{k}_0)$,[2] which is a consequence of the so-called reciprocity theorem first formulated by Lorentz. This theorem predicts that interchanging the spatial locations of the X-ray source and detector cannot vary the intensity of the signal detected (James, 1950). At the same time, the data obtained (Fig. 3) reveal the superiority in intensity of the incoming features over the outgoing ones. This discrepancy needs to be discussed.

At first sight, it seems that the intensity asymmetry relative to the inversion of q_x can be explained by the corresponding asymmetry of $\Delta V(\mathbf{r})$ or by the fact that a normal to the interfaces of layers and the [001] direction can be slightly mismatched. But such disturbances must cause, in particular, essential asymmetry in intensity of the quasi-Bragg scattering, which is not observed. Moreover, such explanations predict that sample rotation around the z axis through 180° must invert the maps relative to the q_x direction. But we find that this rotation does not cause any essential changes in the maps. The incoming features were already observed to be more intense compared to the corresponding outgoing features. Maximal remarkable changes in intensity of the quasi-Bragg scattering only near the satellite were observed when the rotation angle was about ±90°, which corresponds to the case when the terraces are parallel to the specular diffraction plane. Nevertheless, intensity of the quasi-Bragg scattering was observed to be symmetrical in this case, too. Thus, the above reasons cannot explain the discussed asymmetry. In the following discussion, we will suppose that the roughness anisotropy in lateral directions is not important.

The reciprocity theorem is valid in the case of a conservative system and is a sequence of the symmetry of Maxwell's equations relative to time reversal (T invariance). Some processes, which cause the dissipation of coherent wave energy, lead to violation of the reciprocity theorem. Let us consider this effect with the example of photoabsorption. Note that the potential $V_0(z)$ is complex and demands the DWBA modification to be performed. Now the Hamiltonian is non-Hermitian and does not allow one to calculate the scattering amplitude as the simple matrix element (4). Nominally, the scattering amplitude can be written in a form similar to equation (4):

$$\begin{aligned}\Delta f(\mathbf{k}_0 \rightarrow \mathbf{k}_1) &= \frac{1}{4\pi}\langle \tilde{E}, \mathbf{k}_1 - |\Delta V(\mathbf{r})| E, \mathbf{k}_0\rangle \\ &= \frac{1}{4\pi}\int E_{\mathbf{k}_0}(V_0)\tilde{E}_{-\mathbf{k}_1}(V_0^*)\Delta V(\mathbf{r})\,\mathrm{d}\mathbf{r}, \qquad (8)\end{aligned}$$

where the designation $\tilde{E}(V_0^*) = \langle \tilde{E}, \mathbf{k}-|$ means that this function is the *renormalized* solution of wave equation (1) with the complex-conjugate scattering potential $V_0^*(\mathbf{r})$, so that

$$|\tilde{E}, \mathbf{k}_1 -\rangle \rightarrow E^*_{-\mathbf{k}_2} \quad \text{as} \quad \mathrm{Im}(V_0(\mathbf{r})) \rightarrow 0.$$

In spite of the simple form of (8), to obtain in the general case the rigorous expression for the renormalized states $|\tilde{E}, \mathbf{k}_1 -\rangle$ is quite difficult and is beyond the scope of the present work, but in some cases these states can be guessed starting from simple physical reasons.

In the general case, the scattering amplitude (8) is not T invariant but in some cases this symmetry can occur. For example, if the incoming and outgoing angles are far from the Bragg angle, it is possible to ignore the Bragg diffraction. In this case, the states can be written in the following form:

$$\begin{aligned}|E, \mathbf{k}_0\rangle &\cong \exp(ik_{0x}x + ik_{0y}y + ik_{0z}z)\exp(\mu_0 z),\ |\tilde{E}, \mathbf{k}_1 -\rangle \\ &\cong \exp(ik_{1x}x + ik_{1y}y + ik_{1z}z)\exp(\mu_1 z), \qquad (9)\end{aligned}$$

where k_x, k_y and k_z are the real components of $\mathbf{k}$, $\mu_0 \cong \mu/2\sin\theta_0$ and $\mu_1 \cong \mu/2\sin\theta_1$ are positive factors introduced to describe photoabsorption, and μ is the linear coefficient of photoabsorption. Equations (9) allow one to obtain the cross section of quasi-Bragg diffuse scattering, which can be written as

$$\left(\frac{\mathrm{d}\sigma}{\mathrm{d}\Omega}\right)_{\mathrm{QB}} = r_0^2\left|\int \Delta\rho(\mathbf{r})\exp(\mu_0 z + \mu_1 z - i\mathbf{q}\cdot\mathbf{r})\,\mathrm{d}\mathbf{r}\right|^2. \qquad (10)$$

The obtained cross section preserves the discussed symmetry, which has a clear physical meaning. Indeed, let us consider scattering from a defect located at depth h of the object. Amplitude scattering from this defect is proportional to the amplitude of the incident wave, which attenuates owing to photoabsorption at the path length of $h/\sin\theta_0$. The amplitude of the scattered wave attenuates at the path length $h/\sin\theta_1$. The total path length of $h(\sin^{-1}\theta_0 + \sin^{-1}\theta_1)$ is the same for the scattering $\mathbf{k}_0 \rightarrow \mathbf{k}_1$ as well as for the scattering $-\mathbf{k}_1 \rightarrow -\mathbf{k}_0$. Thus, the reciprocity theorem is still true, but only accidentally because the photoabsorption cross section does not depend on the wave propagation direction.

As will be shown below in more detail, the discussed symmetry can vanish if the wave extinction caused by diffraction and scattering is taken into consideration resulting in the appearance of a small term in the exponent of equation (10), which is antisymmetric relative to the index interchange. As a result, the cross section of quasi-Bragg scattering becomes non-T-invariant in the general case, but the symmetry discussed is still true if the electron density $\Delta\rho(\mathbf{r})$ is symmetrical along the z axis. Otherwise, the cross section depends not only on the momentum transfer q_x but on the sign of k_x also. This situation is very similar to the well known effect that intensities of the hkl and $\bar{h}\bar{k}\bar{l}$ reflections can be unequal if the structure factor of this reflection is not symmetrical and photoabsorption is included in the consideration. Thus, the intensity of quasi-Bragg scattering of the maps in Fig. 3 can be asymmetrical relative to the q_z axis but this asymmetry must be weak.

Now, let us show that the discussed effect of asymmetry is more important in the case of incoming and outgoing Bragg features. It is a rather complicated task to obtain analytical

[2] Some asymmetry arises as a result of difference in the limits on integral (4), which is known as a geometry factor. In the case of high-angle diffraction, the influence of this factor is not important.

expressions in this case. Nevertheless, qualitative analysis of the influence of photoabsorption on the intensity of the incoming and outgoing Bragg features can be easily performed. On the assumption of zero photoabsorption, the cross section of the incoming Bragg scattering for an angle of incidence equal to the Bragg angle (θ_B) and outgoing angle equal to some angle θ is exactly equal to the cross section of the outgoing Bragg scattering for an angle of incidence equal to θ and outgoing angle equal to θ_B. At the same time, the depth of penetration of the incident wave and, consequently, the mean path of a scattered X-ray photon through the sample medium are evidently different in these cases. The fact that in the first case this path is essentially smaller allows one to conclude that under absorption conditions the incoming Bragg feature must always be more intense than the outgoing Bragg feature. In the assumption of a thick superlattice (the superlattice thickness is much more than the dynamical extinction depth), it is easy to estimate the degree of asymmetry in the intensities of the incoming and outgoing Bragg features

$$\left(\frac{d\sigma}{d\Omega}\right)_{IBF} \Big/ \left(\frac{d\sigma}{d\Omega}\right)_{OBF} \cong \exp\left[\frac{\mu}{\sin\theta_B}(T-2\tau)\right],$$

where T is the total thickness of the superlattice and τ is the dynamical extinction depth.

Although inclusion of photoabsorption into consideration explains correctly the tendencies of diffuse-scattering behavior, from the point of view of quantitative values this explanation is not adequate. Indeed, the assumption of a thick superlattice is not true in our case,

$$T(\approx 0.4\ \mu m) \leq \tau,$$

and the discussed asymmetry must be weak. Thus, the observed asymmetry (in the case of satellite Bragg reflection the incoming feature intensity is 10–100 times greater than that of the outgoing feature, depending on the value q_z) cannot be explained by photoabsorption.

Aside from photoabsorption, there is another channel of dissipation of the coherent field energy. It is diffuse scattering itself. Note that the reciprocity theorem is a sequence of time-reverse symmetry, but interfacial roughness inevitably is of a statistical nature and any statistical system is irreversible in time. Therefore, in general, the reciprocity theorem cannot be applied to the case when the diffuse scattering is not negligible relative to specular reflection. This fact can be explained more clearly in terms of the multichannel scattering theory. The incoherent diffuse scattering can be considered as an additional reaction channel. At the same time, coherent diffraction can be described by the usual single-channel scattering theory introducing imaginary corrections to the scattering potential, which allows one to take into account dissipation of the coherent field energy through the incoherent diffuse scattering channel. Similar to the case of photoabsorption, these corrections cause violation of the reciprocity theorem.

As was shown above, the asymmetry in intensities of incoming and outgoing features can be caused by the difference in the mean X-ray photon path through the superlattice medium. The same reason is evidently correct for the diffuse-scattering channel of dissipation of coherent wave energy. But similarly to photoabsorption in the approximation of a thin superlattice, the asymmetry caused by this mechanism is also weak. Nevertheless, there is another important source of discussed asymmetry in this case. Before discussion of this, it is necessary to note the following important difference between the photoabsorption and diffuse-scattering channels of dissipation of coherent wave energy. Even in the case of hard photoabsorption, DWBA can be successfully applied to calculate diffuse scattering from a superlattice, which is impossible when energy dissipation is caused by diffuse scattering. When the diffuse-scattering cross section is comparable to or greater than the coherent diffraction cross section, application of DWBA is unjustified because this approximation takes into account only single diffuse-scattering events, whereas, from the experimental point of view, it is impossible to separate the coherent–diffuse and diffuse–diffuse channels. At the same time, diffuse scattering is assumed not to be negligible compared to coherent specular reflection. Indeed, if this last assumption is not true, the symmetry in the intensities of incoming and outgoing Bragg features is provided by the reciprocity theorem. At first sight, the assumption made contradicts the fact that the intensity of specular reflections measured using Cu $K\alpha$ radiation from a conventional source is modeled successfully supposing a perfect structure for the superlattice but, as it is shown below, this contradiction can be solved.

In contrast to photoabsorption, the cross section of diffuse scattering and, accordingly, the imaginary corrections to the scattering potential depend strongly on the wave propagation direction. As was shown above, DWBA predicts that the peak diffuse-scattering cross section is achieved at the Bragg angles of propagation. It gives the key to an explanation why the incoming features dominate over the outgoing features and not the converse. Indeed, if the angle of incidence is far from the Bragg angle, the diffuse-scattering cross section is low and, as a result, the intensity of the outgoing Bragg feature is weak too. Otherwise, when the angle of incidence is equal to the Bragg angle, the diffuse-scattering intensity is high and multiple diffuse-scattering events must be taken into account.[3]

As was shown above, the breakdown of DWBA and the discussed asymmetry are closely related. On the other hand, large-scale roughness is known (de Boer, 1996) to stimulate the violation of Born or DWBA approximations, which can be understood by taking into account that the diffuse-scattering amplitude is proportional to the lateral size of roughness. Let us consider the dependence of diffuse scattering on spatial scales of roughness in more detail. An important diffraction parameter is the average track length along the x axis of the

[3] The discussed strong dependence of the diffuse-scattering cross section on the wave propagation direction is a reason why DWBA can be applied successfully to calculate diffuse scattering except for the cases when the incoming or outgoing angle is equal to the Bragg angle.

X-ray photon in Bragg diffraction. In the approximation of a thin superlattice, its value can be estimated by

$$L_c \sim T \cot\theta_0 \approx 1.5\ \mu\text{m}.$$

Roughness on a scale shorter than this will destroy effectively Bragg diffraction from a superlattice. It is reasonable to call it microroughness.

As for the opposite case, macroroughness will not affect Bragg diffraction. Its influence is restricted by the adiabatic phase shifts in the wavefront in such a manner that the total integrated scattering (TIS) remains unchanged.[4] As a result of phase shifts in the wavefront, the coherent plane wave decays, forming an incoherent quasi-specular reflection as well as an incoming Bragg feature. As was shown in §2, quasi-specular scattering occurs in a very narrow region in the q_x direction of the reciprocal space close to the true specular reflection. From the experimental point of view, it means that to divide the signal measured into the quasi-specular and true specular parts is a sufficiently complicated task. On the other hand, the quasi-specular scattering is caused by the conformal part of the potential ΔV, whereas the Bragg features are caused mainly by the non-conformal part. It is quite evident that macroroughness has completely conformal behavior, which explains the overwhelming domination of quasi-specular scattering over the incoming Bragg scattering. In summary, the above discussion explains why the theoretical calculations of specular intensity based on a highly perfect superlattice structure correspond well to a low-resolution diffraction experiment but, at the same time, the measured scattering can be essentially incoherent.

Comparison of diffraction maps of the basic lattice reflection in Fig. 3(*a*) and its first-order low-angle satellite in Fig. 3(*b*) confirms the conclusion that the asymmetry of intensity of the incoming and outgoing features is caused by the decay of the coherent X-ray field through the diffuse-scattering channel. Indeed, it is possible to show that energy dissipation is lower in the case of the 002 reflection compared to the case of its satellite. As was mentioned above, although the superlattice interfacial roughness caused by terraces is the main source of diffuse scattering in all cases, the mechanism of this phenomenon is different for basic lattice reflections and for satellites. The diffuse scattering around the basic lattice reflection is caused mainly by lateral variations in lattice strain. But the epitaxic lattice mismatch is small in our case. Thus, the diffuse scattering provided by the lattice strain is relatively weak. A different situation is realized in the case of satellites. The interfacial roughness influences the diffraction directly. As a result, the portion of diffuse scattering in TIS increases essentially. The comparison of specular and off-specular scans in Fig. 4 confirms this conclusion. Besides, the data obtained (Fig. 3) allow us to estimate that at least 10–30% of the intensity is diffuse scattering when the angle of incidence is equal to the Bragg angle of the 002 reflection. In the case of the satellite's Bragg angle, the intensity of diffuse scattering exceeds essentially the intensity of the specular reflection.[5] As a result, the domination of diffuse scattering in the case of the satellite explains that intensity asymmetry under discussion is more evident in Fig. 3(*b*) than in Fig. 3(*a*).

Note that features, which are similar to the incoming and outgoing Bragg scattering, around small-angle Bragg reflections from superlattices (Kondrashkina *et al.*, 1997; Stangl *et al.*, 1999), high-angle Bragg reflections (Darhuber *et al.*, 1995) and substrate lattice reflections (Koppensteiner *et al.*, 1994; Darhuber *et al.*, 1995, 1996, 1997; Giannini *et al.*, 1997; Darhuber, Holy *et al.*, 1998; Darhuber, Zhu *et al.*, 1998; Holý, Darhuber, Stangl, Zerlauth *et al.*, 1998; Zhuang *et al.*, 2000) were repeatedly observed. Sometimes these features were explained as an instrumental artifact. Nevertheless, we are sure that our reported features are not an experimental artifact. Firstly, the measurements were accurately performed using calibrated copper foils in order to measure intensity in appropriate tolerance limits of the detector dynamical range. Secondly, mapping of the 002 reflection from the origin substrate does not reveal the features that are discussed.

As a rule, in contrast to our data, the features observed in the cited works appeared in diffraction maps as single streaks. In this connection, it is necessary to mark the importance of spatial coherence of the incident X-ray beam for the Bragg diffraction from multilayers and superlattices (Sinha *et al.*, 1998; Chernov *et al.*, 2002). Spatial coherence of the incident beam increases with the length scales of roughness that are involved in diffraction. In turn, this long-scale roughness causes further increase of the diffuse-scattering cross section. For example, in our case the value of vertical (in the specular diffraction plane) transverse coherence of the incident beam was about 5 μm. It corresponds to the fact that the size in the x direction of the coherently irradiated area was about 20 μm, which is a rather modest value. Thus, it is reasonable to expect that data obtained using SR sources with better spatial coherence can reveal stronger domination of the incoming diffuse-scattering features. Besides, the 002 reflection studied in this work has a low structure factor. Hence, the diffuse-scattering cross section is small, too. It is another reason that allows us to observe the diffuse-scattering fine structure as cross hairs of the incoming and outgoing streaks.

5. Conclusions

In conclusion, we have observed experimentally the resonant features of X-ray diffuse scattering from the AlAs/GaAs superlattice when the incoming or outgoing angle is nearly equal to the Bragg angle of the wide-angle reflections from the superlattice or substrate. The degree of domination in intensity of the incoming feature over the outgoing one was shown

[4] The discussed situation is very similar to the case when a normally incident plane wave penetrates an inhomogeneous non-absorptive plate. Although the total intensity of the output beam in this case is equal to the intensity of the primary beam, the output beam can be completely incoherent.

[5] Note that the TIS dependence *versus* the incoming angle, which can be obtained from our data (Fig. 3), corresponds well to a reflectivity curve calculated using the model of the structurally perfect sample.

to indicate the decay rate of the coherent X-ray field through the diffuse-scattering channel.

The authors thank A. N. Artyushin and I. B. Khriplovich for useful discussions, the personnel of the Siberian Synchrotron Radiation Center headed by G. N. Kulipanov, and experimenters at the VEPP-3 storage ring for help and support. This study was supported by the Russian Foundation for Basic Research, Grant No. 03-02-16259.

References

Andreev, A. V., Michette, A. G. & Renwick, A. (1988). *J. Mod. Opt.* **35**, 1667–1688.
Boer, D. K. G. de (1996). *Phys. Rev. B*, **53**, 6048–6064.
Bruson, A., Dufour, C., George, B., Vergant, M., Marchai, G. & Mangin, Ph. (1989). *Solid State Commun.* **71**, 1045–1050.
Chernov, V. A., Chkhalo, E. D., Kovalenko, N. V. & Mytnichenko, S. V. (2000). *Nucl. Instrum. Methods Phys. Res. A*, **448**, 276–281.
Chernov, V. A., Kondratiev, V. I., Kovalenko, N. V., Mytnichenko, S. V. & Zolotarev, K. V. (2002). *J. Appl. Phys.* **92**, 7593–7598.
Clarke, J., Pape, I., Tanner, B. K. & Wormington, M. (1999). *J. Phys. Condens. Matter*, **11**, 2661–2668.
Darhuber, A. A., Holy, V., Bauer, G., Wang, P. D., Song, Y. P., Sotomayor Torres, C. M. & Holland, M. C. (1996). *Physica (Utrecht)*, B**227**, 11–16.
Darhuber, A. A., Holy, V., Schittenhelm, P., Stangl, J., Kegel, I., Kovats, Z., Metzger, T. H., Bauer, G., Abstreiter, G. & Grübel, G. (1998). *Physica (Utrecht)*, E**2**, 789–793.
Darhuber, A. A., Holy, V., Stangl, J., Bauer, G., Krost, A., Heinrichsdorff, F., Grundman, M., Bimberg, D., Ustinov, V. M., Kop'ev, P. S., Kosogov, A. O. & Werner, P. (1997). *Appl. Phys. Lett.* **70**, 955–957.
Darhuber, A. A., Koppensteiner, E., Bauer, G., Wang, P. D., Song, Y. P., Sotomayor Torres, C. M. & Holland, M. C. (1995). *Appl. Phys. Lett.* **66**, 947–949.
Darhuber, A. A., Zhu, J., Holý, V., Stangl, J., Mikulík, P., Brunner, K., Abstreiter, G. & Bauer, G. (1998). *Appl. Phys. Lett.* **73**, 1535–1537.
Giannini, C., De Riccardis, M. F., Passaseo, A., Tapfer, L. & Peluso, T. (1997). *Appl. Surf. Sci.* **115**, 211–216.
Gibaud, A., Cowley, R. A., McMorrow, D. F., Ward, R. C. C. & Wells, M. R. (1993). *Phys. Rev. B*, **48**, 14463–14471.
Gullikson, E. M., Stearns, D. G., Gaines, D. P. & Underwood, J. H. (1997). *Proc. SPIE*, Vol. 3113–55.
Headrick, R. L., Baribeau, J.-M. & Strausser, Y. E. (1995). *Appl. Phys. Lett.* **66**, 96–98.
Holý, V. & Baumbach, T. (1994). *Phys. Rev. B*, **49**, 10668–10676.
Holý, V., Darhuber, A. A., Stangl, J., Bauer, G., Nützel, J. & Abstreiter, G. (1998). *Phys. Rev. B*, **57**, 12435–12442.
Holý, V., Darhuber, A. A., Stangl, J., Zerlauth, S., Schäffler, F., Bauer, G., Darowski, N., Lübbert, D., Pietsch, U. & Vávra, I. (1998). *Phys. Rev. B*, **58**, 7934–7943.
Holý, V., Stangl, J., Springholz, G., Pinczolits, M., Bauer, G., Kegel, I. & Metzger, T. H. (2000). *Physica (Utrecht)*, B**283**, 65–68.
James, R. W. (1950) *The Optical Principles of the Diffraction of X-rays.* London: Bell.
Jenichen, B., Stepanov, S. A., Brar, B. & Kroemer, H. (1996). *J. Appl. Phys.* **79**, 120–124.
Jergel, M., Holý, V., Majková, E., Luby, Š. & Senderák, R. (1995). *J. Phys. D. Appl. Phys.* **28**, A241–A242.
Kaganer, V. M., Stepanov, S. A. & Kohler, R. (1995). *Phys. Rev. B*, **52**, 16369–16372.
Kondrashkina, E. A., Stepanov, S. A., Opitz, R., Schimidbauer, M., Kohler, R., Hey, R., Wassermeier, M. & Novikov, D. V. (1997). *Phys. Rev. B*, **56**, 10469–10482.
Kopecky, M. (1995). *J. Appl. Phys.* **77**, 2380–2387.
Koppensteiner, E., Hamberger, P., Bauer, G., Holy, V. & Kasper, (1994). *Appl. Phys. Lett.* **64**, 172–174.
Kortright, J. B. (1991). *J. Appl. Phys.* **70**, 3620–3625.
Kortright, J. B. & Fischer-Colbrie, A. (1987). *J. Appl. Phys.* **61**, 1130–1133.
Salditt, T., Lott, D., Metzger, T. H., Peisl, J., Vignaud, G., Legrand, J. F., Grübel, G., Høghøi, P. & Schärpf, O. (1996). *Physica (Utrecht)*, B**221**, 13–17.
Salditt, T., Metzger, T. H., Brandt, Ch., Klemradt, U. & Peisl, J. (1995). *Phys. Rev. B*, **51**, 5617–5627.
Salditt, T., Metzger, T. H. & Peisl, J. (1994). *Phys. Rev. Lett.* **73**, 2228–2231.
Salditt, T., Metzger, T. H., Peisl, J., Reinker, B., Moske, M. & Samwer, K. (1995). *Europhys. Lett.* **32**, 331–336.
Savage, D. E., Kleiner, J., Schimke, N., Phang, Y.-H., Jankowski, T., Jacobs, J., Kariots, R. & Lagally, M. G. (1991). *J. Appl. Phys.* **69**, 1411–1417.
Sinha, S. K., Sanyal, M. K., Satija, S. K., Majkrzak, C. F., Neumann, D. A., Homma, H., Szpala, S., Gibaud, A. & Morkoc, H. (1994). *Physica (Utrecht)*, B**198**, 72–77.
Sinha, S. K., Sirota, E. B., Garoff, S. & Stanley, H. B. (1988). *Phys. Rev. B*, **38**, 2297–2311.
Sinha, S. K., Tolan, M. & Gibaud, A. (1998). *Phys. Rev. B*, **57**, 2740–2758.
Stangl, J., Holy, V., Grim, J., Bauer, G., Zhu, J., Brunner, K., Abstreiter, G., Kienzle, O. & Ernst, F. (1999). *Thin Solid Films*, **357**, 71–75.
Stearns, D. G. (1992). *J. Appl. Phys.* **71**, 4286–4298.
Taylor, J. R., (1972). *Scattering Theory. The Quantum Theory on Nonrelativistic Collisions.* New York: John Wiley.
Zhuang, Y., Pietsch, U., Stangl, J., Holý, V., Darowski, N., Grenzer, J., Zerlauth, S., Schäffler, F. & Bauer, G. (2000). *Physica (Utrecht)*, B**283**, 130–134.